Title
Relationship Between [18F]FDOPA PET Uptake, Apparent Diffusion Coefficient (ADC), and Proliferation Rate in Recurrent Malignant Gliomas.

Permalink
https://escholarship.org/uc/item/6j6650t8

Journal
Molecular imaging and biology, 17(3)

ISSN
1536-1632

Authors
Karavaeva, Elena
Harris, Robert J
Leu, Kevin
et al.

Publication Date
2015-06-01

DOI
10.1007/s11307-014-0807-3

Peer reviewed

MOLECULAR IMAGING AND BIOLOGY

World Molecular Imaging Society

esmi

RESEARCH ARTICLE

Relationship Between [18F]FDOPA PET Uptake, Apparent Diffusion Coefficient (ADC), and Proliferation Rate in Recurrent Malignant Gliomas

Elena Karavaeva,[1] Robert J. Harris,[1,2] Kevin Leu,[1,3] Maryam Shabihkhani,[4]
William H. Yong,[4] Whitney B. Pope,[1] Albert Lai,[5] Phioanh L. Nghiemphu,[5]
Linda M. Liau,[6] Wei Chen,[7] Johannes Czernin,[7] Timothy F. Cloughesy,[5]
Benjamin M. Ellingson[1,2,3]

[1]Department of Radiological Sciences, David Geffen School of Medicine, University of California Los Angeles, 924 Westwood Blvd, Suite 615, Los Angeles, CA, 90024, USA
[2]Department of Biomedical Physics, David Geffen School of Medicine, University of California Los Angeles, Los Angeles, CA, USA
[3]Department of Bioengineering, David Geffen School of Medicine, University of California Los Angeles, Los Angeles, CA, USA
[4]Department of Pathology and Laboratory Medicine, David Geffen School of Medicine, University of California Los Angeles, Los Angeles, CA, USA
[5]Department of Neurology, David Geffen School of Medicine, University of California Los Angeles, Los Angeles, CA, USA
[6]Department of Neurosurgery, David Geffen School of Medicine, University of California Los Angeles, Los Angeles, CA, USA
[7]Department of Pharmacology and Molecular Medicine, David Geffen School of Medicine, University of California Los Angeles, Los Angeles, CA, USA

Abstract

Purpose: Diffusion magnetic resonance imaging (MRI) and 6-[18F]fluoro-L-dopa ([18F]FDOPA) positron emission tomography (PET) are used to interrogate malignant tumor microenvironment. It remains unclear whether there is a relationship between [18F]FDOPA uptake, diffusion MRI estimates of apparent diffusion coefficient (ADC), and mitotic activity in the context of recurrent malignant gliomas, where the tumor may be confounded by the effects of therapy. The purpose of the current study is to determine whether there is a correlation between these imaging techniques and mitotic activity in malignant gliomas.
Procedures: We retrospectively examined 29 patients with recurrent malignant gliomas who underwent structural MRI, diffusion MRI, and [18F]FDOPA PET prior to surgical resection. Qualitative associations were noted, and quantitative voxel-wise and median measurement correlations between [18F]FDOPA PET, ADC, and mitotic index were performed.

Results: Areas of high [^{18}F]FDOPA uptake exhibited low ADC and areas of hyperintensity T2/fluid-attenuated inversion recovery (FLAIR) with low [^{18}F]FDOPA uptake exhibited high ADC. There was a significant inverse voxel-wise correlation between [^{18}F]FDOPA and ADC for all patients. Median [^{18}F]FDOPA uptake and median ADC also showed a significant inverse correlation. Median [^{18}F]FDOPA uptake was positively correlated, and median ADC was inversely correlated with mitotic index from resected tumor tissue.
Conclusions: A significant association may exist between [^{18}F]FDOPA uptake, diffusion MRI, and mitotic activity in recurrent malignant gliomas.

Key words: Diffusion MRI, [^{18}F]FDOPA PET, Malignant glioma, Proliferation, ADC

Introduction

G liomas are a common type of neuroepithelial tumor occurring during adulthood. Diffuse astrocytomas, anaplastic astrocytomas, and glioblastoma multiforme (GBM) are the most common neuroepithelial tumors, with an annual age-adjusted incidence of approximately 4.1 per 100,000 people in the USA [1]. Malignant gliomas, which constitute World Health Organization [WHO] grade III and IV gliomas, are rapidly growing and are uniformly fatal. Despite the recent advances in neurosurgery and adjuvant therapies, the median survival of patients diagnosed with gliomas WHO grades III–IV has improved only slightly and remains relatively poor.

Currently, contrast-enhanced magnetic resonance imaging (CE-MRI) plays a significant role in the evaluation of therapeutic response in recurrent malignant gliomas; however, contrast enhancement with gadolinium is relatively nonspecific for mitotically active tumor. Instead, the degree of contrast enhancement is dependent on the increased permeability of the blood-brain barrier (BBB) from angiogenesis that accompanies aggressive tumor. Because of this nonspecificity, alterations in enhancing tumor on CE-MRI can occur for a variety of reasons unrelated to growing tumor, including after radiation or immunotherapy. Additionally, CE-MRI remains insensitive to subclinical changes that may occur within the tumor, such as changes in metabolism, cellularity, or proliferation rate. Therefore, advanced imaging techniques have been explored as possible methods for interrogating the internal biology of malignant gliomas.

Diffusion MRI and amino acid positron emission tomography (PET) have been proposed as techniques that can provide noninvasive, spatially specific information about tumor cellularity and metabolism, respectively. For example, diffusion MRI estimation of the apparent diffusion coefficient (ADC), a measure of the magnitude of water diffusion within a tissue, has been shown to be negatively correlated with tumor cell density [2–9], presumably due to an increase in boundaries to diffusion within tightly packed tumors leading to a decrease in water mobility. Additionally, studies have shown that changes in ADC are predictive of response to therapy [6, 10–15], where

increasing ADC is reflective of tumor cell destruction in successful cytotoxic therapy and a decrease in ADC may be attributed to nonresponding, growing tumor. Despite initial studies showing a relationship between tumor cellularity and ADC, no studies have examined whether ADC estimates are reflective of mitotically active tumor cell density or whether ADC is sensitive to all cell types.

Amino acid PET techniques, including the use of 6-[^{18}F]fluoro-L-dopa ([^{18}F]FDOPA), have been shown to be beneficial for identifying metabolically active tumor [16–18]. Amino acid transport is increased in malignant cells [19, 20], which is hypothesized to be due the net result of increased demand for amino acids for amino acid synthesis for proliferation [21, 22], transamination, and transmethylation [23, 24]; the use of amino acids as glutamine for fuel [25]; and as precursors for other biochemical syntheses. Previous studies have shown that there to be a relationship between [^{18}F]FDOPA uptake and mitotic activity in newly diagnosed tumors; however, this relationship is less clear in the recurrent setting where uptake may be influenced by other factors including inflammatory processes, such as sarcoidosis [26] and brain abscesses [27], and it may be difficult to differentiate recurrent tumor from background tissue in many cases [28].

It remains unclear whether there is a relationship between [^{18}F]FDOPA uptake, diffusion MRI estimates of ADC, and mitotic activity in the context of recurrent malignant gliomas, where the tumor microenvironment may be confounded by the effects of treatment. In the current retrospective study, we examined 29 patients with recurrent malignant gliomas who underwent MRI and [^{18}F]FDOPA PET prior to surgical resection in order to determine whether there is a spatial correlation between these imaging techniques, suggesting that they may provide similar information, and whether these measurements reflect the underlying mitotic activity of these tumors.

Materials and Methods

Patients

A total of 110 retrospective enrolled patients with malignant gliomas (WHO III–IV) received [^{18}F]FDOPA PET scans for suspected tumor

recurrence since 2006. A total of 29 out of these 110 patients had (1) preoperative [^{18}F]FDOPA PET scans *and* high-quality diffusion MR images within 2.5 months of surgical resection, (2) treatment and subsequent failure of concurrent radiation and temozolomide followed by adjuvant temozolomide, (3) suspected recurrence more than 12 weeks from end of concurrent radiochemotherapy, (4) no bevacizumab or immunotherapies prior to PET and MRI, and (5) surgical resection as a result of suspected recurrent disease with no notable change in tumor histology. There were 22 men and 7 women, with a mean age of 49.4±12.7 years, ranging from 23 to 72 years. By the time of this study, 22 patients have died and 7 remain alive. The time between preoperative [^{18}F]FDOPA PET acquisition and subsequent histological diagnosis was 1.14±0.69 months. Twenty patients were diagnosed with GBM (WHO grade IV), and 9 patients were diagnosed with WHO grade III tumors (three patients with anaplastic oligodendroglioma, five patients with anaplastic astrocytoma, and one patient with anaplastic mixed glioma). All patients presented with tumor recurrence at the time of PET and MRI and underwent subsequent surgical resection. In addition to surgery, all patients had received radiation and chemotherapy prior to recurrence. The median time from completion of radiotherapy to PET imaging was 12.6 months. This prospective analytical study was conducted after obtaining the approval of the University of California, Los Angeles, Office for Protection of Research Subjects. Written informed consent was obtained from all patients. Additional patient characteristics are described in Table 1.

6-[^{18}F]Fluoro-L-Dopa Positron Emission Tomography

[^{18}F]FDOPA PET scans were acquired for all 29 patients using a high-resolution full-ring PET scanner (ECAT-HR; CTI/MIMVista). Patients were instructed to fast for more than 4 h prior to PET acquisition. [^{18}F]FDOPA was synthesized and injected intravenously; injected doses averaged 125.4±22.9 MBq, 1.54±0.37 Bq/kg. A CT scan was acquired prior to PET for attenuation correction. Three-dimensional [^{18}F]FDOPA emission data were acquired 10 min after radiotracer injection for a total of 30 min. Data was integrated between 10 and 30 min from injection to obtain a 20-min static [^{18}F]FDOPA images following reconstruction. PET images were reconstructed using an ordered-subset expectation maximization iterative reconstruction algorithm consisting of six iterations with eight subsets [29, 30]. Lastly, a Gaussian filter with a full width at half maximum of 4 mm was applied. The resulting voxel sizes were 1.34 mm×1.34 mm×3 mm for [^{18}F]FDOPA PET standard uptake volume (SUV) maps.

Magnetic Resonance Imaging

All MR data were collected on a 1.5T MR system (General Electric Medical Systems or Siemens Medical). Standard anatomical MRI sequences included axial T1-weighted, T2-weighted, and fluid-attenuated inversion recovery (FLAIR) images. In addition, gadopentetate dimeglumine-enhanced (Magnevist; 0.1 mmol/kg) axial and coronal T1-weighted images (T1 + C) were acquired after contrast injection.

Diffusion tensor images (DTIs) were collected on a 1.5T MR system (General Electric Medical Systems or Siemens Medical) in 20 equidistant diffusion-sensitizing directions with b=1000 s/mm^2, along with a single b=0 s/mm^2 image, with a resolution of 2 mm×2 mm×2 mm. The diffusion tensor was estimated using *TrackVis* (Martinos Center for Biomedical

Imaging/MGH; http://trackvis.org), and mean diffusivity maps were used as estimates of ADC.

Image Registration

All PET and MRI images for were registered to the post-contrast T1-weighted images for each respective patient using a 12-degree of freedom affine transformation and a mutual information cost function. (FSL; FMRIB, Oxford, UK; http://www.fmrib.ox.ac.uk/fsl/). If required, manual alignment was subsequently performed (*tkregister2*, *Freesurfer*; surfer.nmr.mgh.harvard.edu; Massachusetts General Hospital, Harvard Medical School). To register the ADC maps, we rigidly aligned b0 images acquired during DTI sequence to the CE-MRI using the FSL Linear Image Registration Tool. Regions of T2 or FLAIR signal abnormality as well as regions of T1 contrast enhancement were contoured and masked using a semiautomated thresholding technique for each patient. Radiotracer concentration within the ROIs was normalized to the injected dose per kilogram of patient's body weight to derive SUV. Additionally, PET SUV images for each patient were normalized to the areas of normal-appearing basal ganglia selected from the corresponding aligned MR images. [^{18}F]FDOPA PET uptake higher than the basal ganglia has been shown to be predictive of active tumor with high sensitivity and specificity [31]. The volume of tumor was defined as the area of contrast enhancement on CE-MR images. On FLAIR sequences, the region of abnormally increased signal intensity encompassing both the volumes of enhancing tumor and surrounding edema were contoured. Necrotic areas were excluded from the analysis. We chose to include contrast-enhancing tumor within our FLAIR-defined regions of interest in order to ensure a wide range of both PET and ADC measurements for correlation purposes (i.e., to make sure that the analysis contains both aggressive or enhancing tumor as well as edematous tissues, which both appear abnormal on FLAIR). Median SUVs of [^{18}F]FDOPA along with median ADC values were calculated in the regions of contrast enhancement on T1 image sequences and in the areas of T2 or FLAIR abnormalities using normalized PET data.

Histopathology and Immunohistochemistry

A total of 20 of the 29 patients had tissue available for evaluation. All tissue was obtained from contrast-enhancing regions *via* biopsy and under image guidance, but stereospecificity of the tissue was not retained for precise matching with imaging data. All tumors were graded using the WHO grading system and stained for Ki-67 expression. The samples from the surgery were divided into different blocks. Histology section and microscopic examination are performed over all those different blocks. Sections of 5 μm were cut from formalin-fixed paraffin-embedded (FFPE) blocks of tumors (known to have tumor) and processed for immunohisto-chemical detection of Ki-67. Appropriate positive and negative controls were used to ensure good immunohistochemical staining. Measurement of proliferation from Ki-67-stained slides was performed manually by board certified neuropathologists. For manual scoring in each specimen, the number of tumor cells with distinct nuclear staining of Ki-67 as well as the total number of cells was manually counted in 20 ×200 fields reflecting the areas of highest Ki-67 labeling from contrast-enhancing regions obtained from resected tumor tissue under image guidance. The percentages of Ki-67-immunopositive cells were calculated for each field, and the average of these percentages was used for analysis.

Table 1. Patient characteristics

Patient no.	Gender	Age	Weight (kg)	KPS	Tumor	WHO grade	Prior recurrences	Time between PET and histology (months)	Enhancing tumor volume (cc)	T2/FLAIR volume (cc)
1	M	66	92.986	60	AO	3	1	0.07	6.21	71.01
2	M	47	80.910	90	GBM	4	1	0.16	2.91	45.34
3	M	45	88.984	90	GBM	4	1	0.2	12.19	46.21
4	M	72	80.000	60	GBM	4	1	0.23	17.60	106.39
5	M	59	86.260	90	GBM	4	1	0.43	0.40	20.42
6	F	49	62.000	80	GBM	4	2	0.49	41.07	241.22
7	F	45	59.029	90	GBM	4	2	0.49	20.46	65.27
8	F	56	112.500	60	AO	3	8	0.52	43.70	94.58
9	M	41	88.984	100	AO	3	1	0.52	2.01	32.35
10	F	41	58.112	80	GBM	4	2	0.75	11.47	24.03
11	M	56	98.518	80	GBM	4	1	0.79	2.36	68.49
12	M	45	98.064	100	AMG	3	1	0.89	0.13	10.96
13	M	61	81.720	80	GBM	4	1	0.92	1.54	29.33
14	M	43	85.352	90	GBM	4	1	1.11	0.82	3.10
15	M	66	118.040	90	GBM	4	1	1.15	1.23	1.16
16	M	47	63.560	90	AO	3	3	1.15	0.11	18.23
17	M	31	94.886	100	GBM	4	1	1.34	24.27	19.38
18	M	41	95.340	90	GBM	4	2	1.34	8.83	45.37
19	F	65	59.928	60	GBM	4	2	1.34	13.30	48.98
20	M	68	117.934	90	GBM	4	1	1.44	6.68	43.58
21	M	62	95.340	90	GBM	4	1	1.51	10.60	64.84
22	M	42	75.300	90	AA	3	1	1.54	5.69	14.06
23	M	62	99.880	90	GBM	4	2	1.9	0.30	0.93
24	F	41	72.640	100	AA	3	1	1.93	6.93	95.11
25	M	37	78.542	80	GBM	4	1	2.07	24.69	229.77
26	M	23	89.000	90	AA	3	1	2.1	0.24	21.61
27	M	45	85.000	90	AA	3	1	2.16	1.68	9.87
28	F	51	59.020	90	GBM	4	3	2.16	6.33	32.15
29	M	26	62.270	100	GBM	4	1	2.33	0.93	1.17

M male, *F* female, *AO* anaplastic oligodendroglioma, *AA* anaplastic astrocytoma, *KPS* Karnofsky performance score

Statistical Analysis

Voxel-by-voxel correlation between [^{18}F]FDOPA uptake and ADC was performed for FLAIR-hyperintense regions in each patient at the resolution of the [^{18}F]FDOPA PET scans to examine general trends between these two modalities. FLAIR-hyperintense regions were chosen in order to include regions of contrast-enhancing tumor, peritumoral edema, and nonenhancing tumor. Regions of necrosis were excluded from the analysis. The slopes of the regression lines comparing [^{18}F]FDOPA-normalized SUV and [^{18}F]FDOPA-normalized ADC for each patient were then grouped to determine whether these were significantly different from zero using a t test. Additionally, the correlations between median [^{18}F]FDOPA uptake, median ADC values, and tumor proliferation (KI-67) were calculated using linear regression analysis. All statistical tests were performed using GraphPad Prism, version 4.0 (GraphPad Software).

Results

In general, areas of elevated [^{18}F]FDOPA uptake within contrast-enhancing tumor regions appeared to also have a low ADC on diffusion MRI (Fig. 1), consistent with the hypothesis that regions of low ADC may reflect active tumor. Additionally, regions within FLAIR-hyperintense regions exhibiting low [^{18}F]FDOPA uptake relative to the basal ganglia demonstrated elevated ADC, consistent with a lower tumor cellularity in these regions. This was expected, since FLAIR-hyperintense regions can contain a mixture of peritumoral edema as well as nonenhancing tumor.

The association between [^{18}F]FDOPA uptake and ADC was verified by examining the voxel-wise correspondence within each patient. As illustrated in Fig. 2a–h, we observed a statistically significant correlation between [^{18}F]FDOPA uptake and ADC for all 29 patients examined (Pearson's correlation coefficient, $P<0.05$). Interestingly, we also observed deviation of this linear trend for regions with low ADC in many cases. In particular, many patients demonstrated a spike in [^{18}F]FDOPA uptake in regions with a low, but constant ADC. These trends may suggest a practical minimum ADC within the tumor, perhaps corresponding to maximum cell packing, regardless of metabolic activity. Generally speaking, we observed a significant negative correlation between [^{18}F]FDOPA uptake and ADC for each patient within FLAIR-hyperintense regions (Fig. 2i; mean slope=-0.2523 ± 0.0167 SEM [^{18}F]DOPA-normalized SUV/[μm^2/ms]; t test, observed slope vs. slope=0; $P<0.0001$). Consistent with voxel-wise trends within the tumor, median [^{18}F]FDOPA uptake relative to the basal ganglia, and median ADC calculated in each patient within FLAIR-hyperintense regions exhibited a significant negative correlation (Fig. 3a; slope=-0.3609 ± 0.1227 SEM [^{18}F]DOPA-normalized SUV/[μm^2/ms]; $R^2=0.4240$, $P=0.0006$). Additionally, we observed a significant, but relatively weak
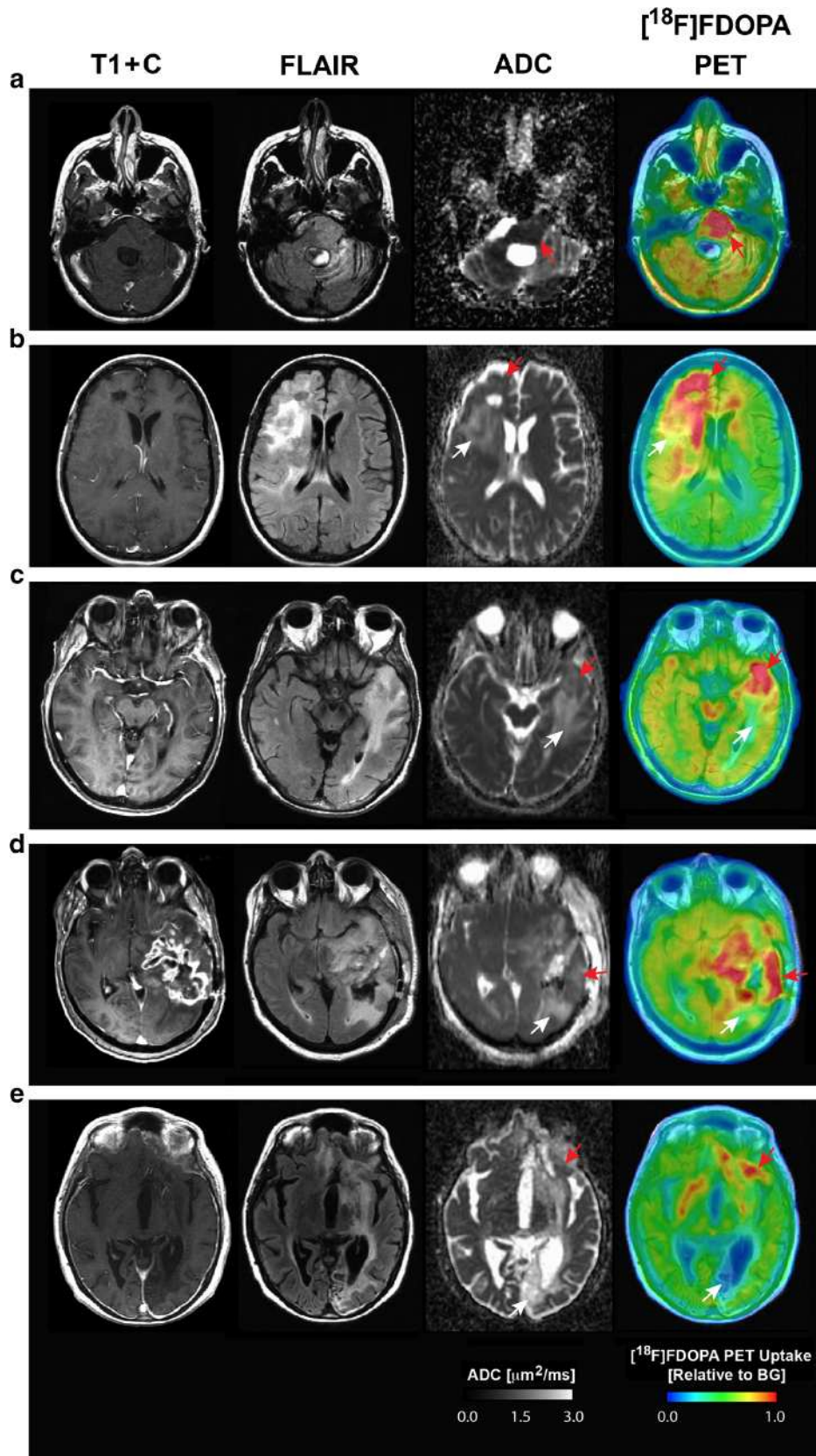
Fig. 1   Post-contrast T1-weighted images, T2-weighted FLAIR, diffusion MRI estimates of ADC, and [18F]FDOPA PET SUV images in five patients (a–e) with malignant gliomas. Regions of high [18F]FDOPA uptake appear to be spatially correlated with areas of relatively low ADC within FLAIR-hyperintense regions (red arrows), whereas areas of low [18F]FDOPA uptake appear to be localized to areas of high ADC (white arrows).

negative trend between the median [18F]FDOPA uptake and median ADC within areas of contrast-enhancing tumor (Fig. 3b; slope=-0.7648 ± 0.3083 SEM [18F]FDOPA-normalized SUV/[μm^2/ms]; R^2=0.2658, P=0.0239).

Consistent with the hypothesis that [18F]FDOPA PET uptake reflects general mitotic activity of the tumor, we observed a significant positive correlation between average mitotic activity within resected enhancing tumor, as estimated from manual counts of average Ki-67-positive cells per ×20 field and median [18F]FDOPA uptake within areas of contrast enhancement (Fig. 3c; slope=61.63 ± 27.24 SEM Ki-67-positive cells per ×200 field per normalized [18F]FDOPA SUV; R^2=0.2215, P=0.0362). No statistically significant correlation was observed between [18F]FDOPA PET SUV and mitotic activity when patients were split into WHO IV (N=15, R^2=0.2231, P=0.0754) and WHO III (N=5, R^2=0.2570, P=0.3834) grade tumors. Additionally, we observed a significant linear correlation between mitotic activity within the enhancing tumor and median ADC within enhancing tumor (Fig. 3d; slope=-86.85 ± 32.84 Ki-67-positive cells per ×200 field per [μm^2/ms]; R^2=0.2799,

P=0.0165). The correlation between ADC and mitotic activity was statistically significant for WHO III tumors (N=5, R^2=0.9828, P=0.001) but only trended toward significance in WHO IV tumors (N=15, R^2=0.2512, P=0.057). Important to note is that these trends were relatively weak and there appeared to be a subset of data exhibiting a relatively strong association between imaging measurements and mitotic activity (arrows in Fig. 3c, d), while a few outliers with high focal mitotic activity may have skewed the general associations observed.

Discussion

Histology of excised tissue remains the gold standard for identifying biological characteristics pertinent to the aggressiveness and treatment sensitivity of the tumor, including estimates of cellular proliferation. The antigen Ki-67 has been reported as the most reliable marker for cellular proliferation because of its expression in almost all phases of the cell cycle, except for the G0 phase [32, 33]. Therefore, a noninvasive method of assessing glioma proliferation
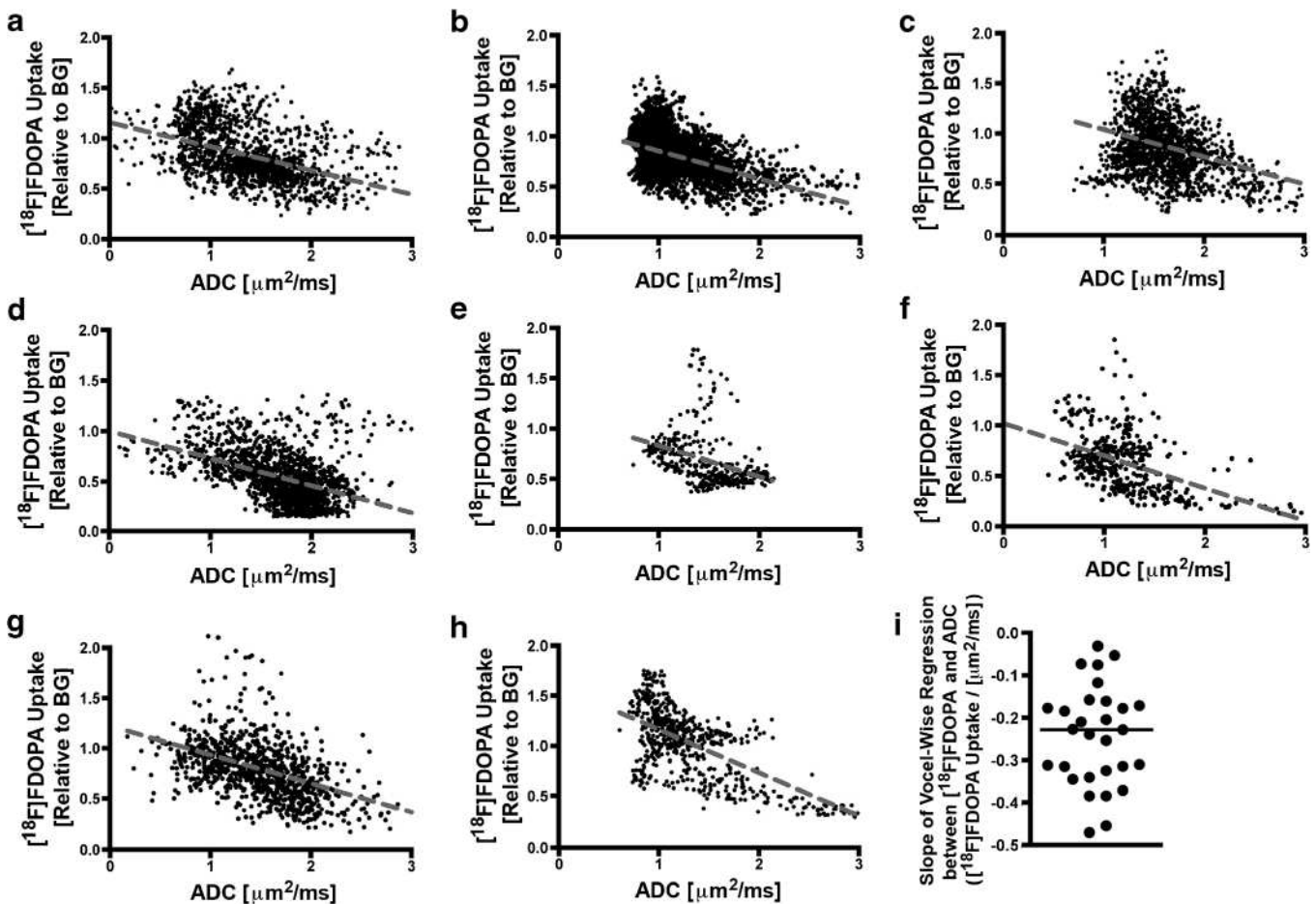

Fig. 2 Voxel-by-voxel correspondence between [18F]FDOPA PET uptake and ADC in T2/FLAIR-hyperintense regions for eight representative patients (a–h), illustrating a general inverse linear correlation. i Slope of the linear regression line after voxel-wise correlation of [18F]FDOPA uptake and ADC within T2/FLAIR-hyperintense regions in each patient. Mean slope=-0.2523 ± 0.0167 SEM [18F]DOPA-normalized SUV/[μm^2/ms]; t test, observed slope vs. slope=0; $P<0.0001$.
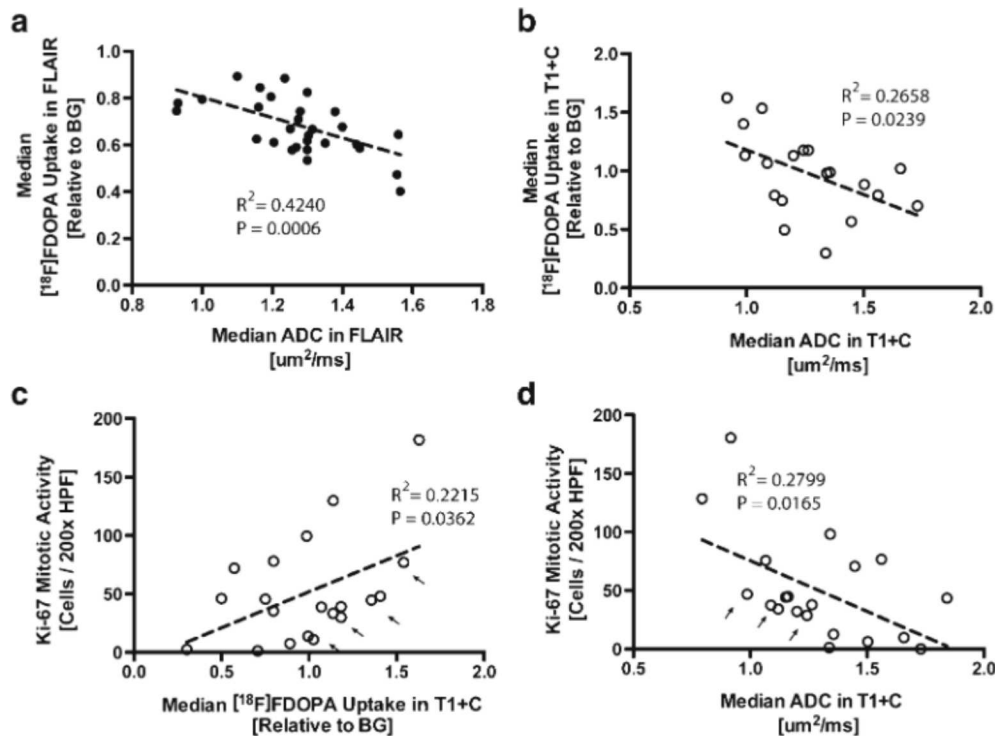
Fig. 3 **a** Correlation between median normalized [¹⁸F]FDOPA SUV and median ADC within T2/FLAIR-hyperintense regions evaluated across all patients (slope=-0.3609 ± 0.1227 SEM [¹⁸F]DOPA-normalized SUV/[μm^2/ms]; R^2=0.4240, P=0.0066). **b** Correlation between median normalized [¹⁸F]FDOPA SUV and median ADC within contrast-enhancing regions evaluated across all patients (slope=-0.7648 ± 0.3083 SEM [¹⁸F]FDOPA-normalized SUV/[μm^2/ms]; R^2=0.2658, P=0.0239). **c** Correlation between median normalized [¹⁸F]FDOPA uptake and mitotic activity (slope=61.63 ± 27.24 SEM Ki-67-positive cells per ×200 field per normalized [¹⁸F]FDOPA SUV; R^2=0.2215, P=0.0362). **d** Correlation between median ADC and mitotic activity (slope=-86.85 ± 32.84 Ki-67-positive cells per ×200 field per [μm^2/ms]; R^2=0.2799, P=0.0165). Arrows highlight a subset of data that appears to exhibit a relatively strong association between imaging measurements and mitotic activity.

should demonstrate an association with mitotic index or proliferation rate as assessed using Ki-67.

Amino acid and amino acid PET tracers are particularly useful for imaging of brain tumors because of their low uptake in normal brain and high uptake in tumor. [¹⁸F]FDOPA is an amino acid tracer for PET synthesized in mammalian cells from L-tyrosine, by the enzyme tyrosine hydroxylase, and is a precursor of the neurotransmitters dopamine, norepinephrine, and epinephrine. [¹⁸F]FDOPA PET is believed to label tumor cells due to increased demand for amino acid synthesis for proliferation [21, 22], transamination, and transmethylation [23, 24]; the use of amino acids as glutamine for fuel [25]; and as precursors for other biochemical syntheses. As such, previous studies have shown that there to be a relationship between [¹⁸F]FDOPA uptake and mitotic activity in newly diagnosed tumors; however, this relationship is less clear in the recurrent setting where uptake may be influenced by other factors including inflammatory processes [28]. Additionally, diffusion MRI has been shown to be negatively correlated with tumor cell density [2–9] and restricted diffusion is thought to occur in the most aggressive areas of the tumor. Despite this association in newly diagnosed tumors, to our knowledge, no studies have explicitly examined whether ADC estimates

are reflective of mitotically active tumor cell density in the context of recurrent malignant gliomas. Thus, we hypothesized that a strong inverse association would exist between [¹⁸F]FDOPA PET uptake and ADC within these tumors and that tumors with elevated [¹⁸F]FDOPA PET and/or low ADC would exhibit the highest mitotic index.

Results from the current study support the hypothesis that high [¹⁸F]FDOPA uptake is generally localized to areas of low ADC and that these results reflect areas of tumor with high mitotic activity in recurrent tumor. The correlation between amino acid PET uptake and proliferation has been well documented in newly diagnosed brain tumors using a variety of amino acid tracers [22, 34–36]; however, this association has not been well established in recurrent tumors. For example, a previous study by Fueger et al. [28] found a correlation between [¹⁸F]FDOPA SUV measurements and the mitotic index in newly diagnosed tumors but failed to find a significant association with recurrent tumors. However, this study (and many other PET studies) only examined a region of interest placed over the area of highest uptake on the PET images and did not examine [¹⁸F]FDOPA uptake localized to areas of contrast enhancement. Therefore, it is conceivable that the current study more concisely captures the metabolic characteristics of the tumor

regions being evaluated *via* histology. Similar to amino acid PET, diffusion MRI estimates of ADC have been shown to be correlated with tumor cellularity [2–9] and mitotic index [37, 38], but again only in newly diagnosed brain tumors. To the best of our knowledge, no studies have observed an association between ADC and mitotic index in recurrent high-grade gliomas.

Voxel-wise correlations between [18F]FDOPA uptake and ADC in the current study suggest a general linear association between these imaging measurements but interestingly also illustrated areas of high [18F]FDOPA uptake with a constant, low ADC. This latter observation is consistent with the hypothesis that there may be a lower limit to tumor ADC and metabolic activity may vary even within these highly dense tumors. It is conceivable that this low ADC limit may possibly reflect the maximum cell packing possible within the respective tumor, and this limit may occur regardless of whether the tumor is actively proliferating.

Study Limitations

There are a few limitations to the current study that should be addressed. First, the current retrospective study lacked a degree of stereospecificity for the histological samples taken; therefore, the correlation between imaging measurements and mitotic index on Ki-67 may be lesser than would be expected with a higher degree of spatial localization. It is important to note that mitotic index measurements were taken from various slides throughout contrast-enhancing tumor regions, which were subsequently correlated with median measurements of imaging features in within the same general areas. Additionally, Ki-67 staining is not necessarily specific to tumor cells undergoing cell proliferation but can also stain other cells that proliferate rapidly, including immune cells. The observed association between [18F]FDOPA uptake and mitotic index in the current study may be associated with both tumor proliferation and treatment-related changes, since elevated [18F]FDOPA uptake can also occur during inflammation.

Conclusion

Regions exhibiting high [18F]FDOPA uptake on PET scans are typically localized to areas of low ADC on diffusion MRI, and these regions typically have a high mitotic index in recurrent malignant gliomas.

References

1. DeAngelis LM (2001) Brain tumors. N Engl J Med 344:114–123
2. Bode MK, Ruohonen J, Nieminen MT, Pyhtinen J (2006) Potential of diffusion imaging in brain tumors: a review. Acta Radiol 47:585–594
3. Ellingson BM, Malkin MG, Rand SD et al (2010) Validation of functional diffusion maps (fDMs) as a biomarker for human glioma cellularity. J Magn Reson Imaging 31:538–548
4. Sugahara T, Korogi Y, Kochi M et al (1999) Usefulness of diffusion-weighted MRI with echo-planar technique in the evaluation of cellularity in gliomas. J Magn Reson Imaging 9:53–60
5. Lyng H, Haraldseth O, Rofstad EK (2000) Measurement of cell density and necrotic fraction in human melanoma xenografts by diffusion weighted magnetic resonance imaging. Magn Reson Med 43:828–836
6. Chenevert TL, Stegman LD, Taylor JM et al (2000) Diffusion magnetic resonance imaging: an early surrogate marker of therapeutic efficacy in brain tumors. J Natl Cancer Inst 92:2029–2036
7. Guo AC, Cummings TJ, Dash RC, Provenzale JM (2002) Lymphomas and high-grade astrocytomas: comparison of water diffusibility and histologic characteristics. Radiology 224:177–183
8. Hayashida Y, Hirai T, Morishita S et al (2006) Diffusion-weighted imaging of metastatic brain tumors: comparison with histologic type and tumor cellularity. AJNR Am J Neuroradiol 27:1419–1425
9. Kinoshita M, Hashimoto N, Goto T et al (2008) Fractional anisotropy and tumor cell density of the tumor core show positive correlation in diffusion tensor magnetic resonance imaging of malignant brain tumors. Neuroimage 43:29–35
10. Chenevert TL, McKeever PE, Ross BD (1997) Monitoring early response of experimental brain tumors to therapy using diffusion magnetic resonance imaging. Clin Cancer Res Off J Am Assoc Cancer Res 3:1457–1466
11. Ross BD, Moffat BA, Lawrence TS et al (2003) Evaluation of cancer therapy using diffusion magnetic resonance imaging. Mol Cancer Ther 2:581–587
12. Moffat BA, Hall DE, Stojanovska J et al (2004) Diffusion imaging for evaluation of tumor therapies in preclinical animal models. Magma 17:249–259
13. Hein PA, Eskey CJ, Dunn JF, Hug EB (2004) Diffusion-weighted imaging in the follow-up of treated high-grade gliomas: tumor recurrence versus radiation injury. AJNR Am J Neuroradiol 25:201–209
14. Asao C, Korogi Y, Kitajima M et al (2005) Diffusion-weighted imaging of radiation-induced brain injury for differentiation from tumor recurrence. AJNR Am J Neuroradiol 26:1455–1460
15. Sundgren PC, Fan X, Weybright P et al (2006) Differentiation of recurrent brain tumor versus radiation injury using diffusion tensor imaging in patients with new contrast-enhancing lesions. Magn Reson Imaging 24:1131–1142
16. Weber WA, Wester HJ, Grosu AL et al (2000) O-(2-[18F]fluoroethyl)-L-tyrosine and L-[methyl-11C]methionine uptake in brain tumours: initial results of a comparative study. Eur J Nucl Med 27:542–549
17. Becherer A, Karanikas G, Szabo M et al (2003) Brain tumour imaging with PET: a comparison between [18F]fluorodopa and [11C]methionine. Eur J Nucl Med Mol Imaging 30:1561–1567
18. Grosu AL, Astner ST, Riedel E et al (2011) An interindividual comparison of O-(2-[18F]fluoroethyl)-L-tyrosine (FET)- and L-[methyl-11C]methionine (MET)-PET in patients with brain gliomas and metastases. Int J Radiat Oncol Biol Phys 81:1049–1058
19. Isselbacher KJ (1972) Sugar and amino acid transport by cells in culture–differences between normal and malignant cells. N Engl J Med 286:929–933
20. Busch H, Davis JR, Honig GR et al (1959) The uptake of a variety of amino acids into nuclear proteins of tumors and other tissues. Cancer Res 19:1030–1039
21. Kato T, Shinoda J, Oka N et al (2008) Analysis of 11C-methionine uptake in low-grade gliomas and correlation with proliferative activity. AJNR Am J Neuroradiol 29:1867–1871
22. Sato N, Suzuki M, Kuwata N et al (1999) Evaluation of the malignancy of glioma using 11C-methionine positron emission tomography and proliferating cell nuclear antigen staining. Neurosurg Rev 22:210–214
23. Chiang PK, Cantoni GL (1977) Activation of methionine for transmethylation. Purification of the S-adenosylmethionine synthetase of bakers' yeast and its separation into two forms. J Biol Chem 252:4506–4513
24. Meyer GJ, Schober O, Hundeshagen H (1985) Uptake of 11C-L- and D-methionine in brain tumors. Eur J Nucl Med 10:373–376
25. Souba WW (1993) Glutamine and cancer. Ann Surg 218:715–728

26. Yamada Y, Uchida Y, Tatsumi K et al (1998) Fluorine-18-fluorodeoxyglucose and carbon-11-methionine evaluation of lymph-adenopathy in sarcoidosis. J Nucl Med 39:1160–1166
27. Floeth FW, Pauleit D, Sabel M et al (2006) ^{18}F-FET PET differentiation of ring-enhancing brain lesions. J Nucl Med 47:776–782
28. Fueger BJ, Czernin J, Cloughesy T et al (2010) Correlation of 6-^{18}F-fluoro-L-dopa PET uptake with proliferation and tumor grade in newly diagnosed and recurrent gliomas. J Nucl Med 51:1532–1538
29. Kinahan PE, Townsend DW, Beyer T, Sashin D (1998) Attenuation correction for a combined 3D PET/CT scanner. Med Phys 25:2046–2053
30. Nuyts J, Michel C, Dupont P (2001) Maximum-likelihood expectation-maximization reconstruction of sinograms with arbitrary noise distribution using NEC-transformations. IEEE Trans Med Imaging 20:365–375
31. Chen W, Silverman DH, Delaloye S et al (2006) ^{18}F-FDOPA PET imaging of brain tumors: comparison study with ^{18}F-FDG PET and evaluation of diagnostic accuracy. J Nucl Med 47:904–911
32. Johannessen AL, Torp SH (2006) The clinical value of Ki-67/MIB-1 labeling index in human astrocytomas. Pathol Oncol Res POR 12:143–147
33. Prayson RA (2005) The utility of MIB-1/Ki-67 immunostaining in the evaluation of central nervous system neoplasms. Adv Anat Pathol 12:144–148
34. Hatakeyama T, Kawai N, Nishiyama Y et al (2008) ^{11}C-methionine (MET) and ^{18}F-fluorothymidine (FLT) PET in patients with newly diagnosed glioma. Eur J Nucl Med Mol Imaging 35:2009–2017
35. Huang MC, Shih YH, Chen MH et al (2005) Malignancy of intracerebral lesions evaluated with ^{11}C-methionine-PET. J Clin Neurosci Off J Neurosurg Soc Australas 12:775–780
36. Kim S, Chung JK, Im SH et al (2005) ^{11}C-methionine PET as a prognostic marker in patients with glioma: comparison with ^{18}F-FDG PET. Eur J Nucl Med Mol Imaging 32:52–59
37. Yuan W, Holland SK, Jones BV et al (2008) Characterization of abnormal diffusion properties of supratentorial brain tumors: a preliminary diffusion tensor imaging study. J Neurosurg Pediatr 1:263–269
38. Gauvain KM, McKinstry RC, Mukherjee P et al (2001) Evaluating pediatric brain tumor cellularity with diffusion-tensor imaging. AJR Am J Roentgenol 177:449–454